2014-11

Finite-element analysis of a piled embankment with reinforcement compared with BS 8006 predictions

ZHUANG, Y

10.1680/geot.14.P.110
Geotechnique
Thomas Telford Ltd.

Zhuang, Y. & Ellis, E. (2014). *Géotechnique* **64**, No. 11, 910–917 [http://dx.doi.org/10.1680/geot.14.P.110]

Finite-element analysis of a piled embankment with reinforcement compared with BS 8006 predictions

Y. ZHUANG* and E. ELLIS†

The British 'Code of practice for strengthened/reinforced soils and other fills' (BS 8006) was substantially revised in 2010, with a further 'Corrigendum' in 2012. Historically, BS 8006 considered arching in a piled embankment, based on an interpretation of the 'Marston' equation. The 2010 revision included an alternative method related to the analysis of arching in a piled embankment, which was proposed by Hewlett and Randolph in 1988, and later itself amended in the 2012 Corrigendum. This contribution considers BS 8006 predictions of reinforcement tension using these methods as a basis for embankment load on the reinforcement, for a wide range of piled embankment geometries. The predictions are compared with results from three-dimensional finite-element analysis, demonstrating encouraging correspondence with the Hewlett and Randolph approach (but noting that the 2010 revision overpredicts the data whereas the 2012 revision underpredicts it). Good predictions of maximum reinforcement sag are also achieved by slight modification of the BS 8006 method.

KEYWORDS: embankments; finite-element modelling; geosynthetics

INTRODUCTION

A piled embankment (Fig. 1(a)) relies on arching of the embankment material to transfer a significant amount of the embankment load directly onto pile caps. The remaining load (e.g. below the arch) is carried by some combination of tensile reinforcement (which is frequently used) and/or the subsoil (if this is realistic/admissible in design).

The British 'Code of practice for strengthened/reinforced soils and other fills' (BS 8006) was substantially revised in 2010 (BSI, 2010). Historically BS 8006 considered arching in a piled embankment based on an interpretation of the 'Marston' equation, and corresponding tension in a single layer of extensible reinforcement near the base of the embankment. The 2010 revision included an alternative method for arching proposed by Hewlett & Randolph (1988), and a new 'minimum limit' on reinforcement tension.

Van Eekelen *et al.* (2011) proposed modification of BS 8006 for piled embankments based on comparison with axisymmetric finite-element (FE) analyses. However, the comparison does not consider the Hewlett and Randolph approach, and the use of axisymmetric FE analysis is questionable. There are other examples in the literature of authors modelling biaxial geogrid reinforcement as an isotropic material (e.g. Liu *et al.*, 2007).

Plaut & Filz (2010), Jones *et al.* (2010) and Halvordson *et al.* (2010) present an interesting comparison of axisymmetric, isotropic and biaxial geogrid reinforcement, respectively. The results indicate considerable variation in the maximum tension, which is observed at the corner of a pile cap. The isotropic model gives a considerable 'spike' in tension at this point. Conversely the axisymmetric model gives very little increase at the edge of the pile cap (noting that a corner is not actually modelled as such). The biaxial geogrid ('cable net') model lies between these two extremes, with a 'moderate' spike in tension at the corner of a pile cap. Although these studies give a good insight into different approaches to modelling of the reinforcement, other aspects of the modelling are somewhat idealised. Most notably embankment loading is

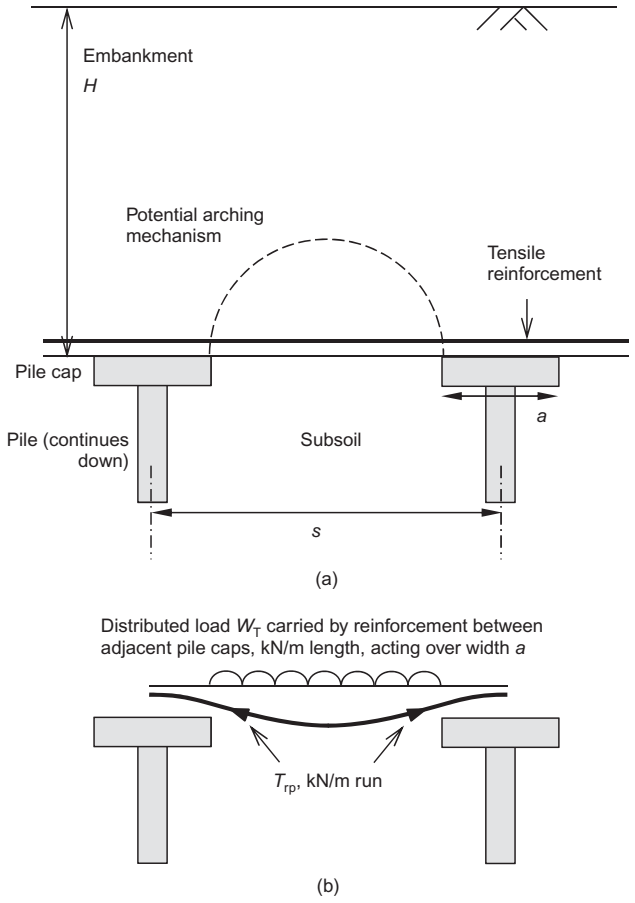

Fig. 1. Section through piled embankment illustrating behaviour and notation: (a) schematic diagram of behaviour and geometry; (b) reinforcement load (W_T) and tension (T_{rp})

Manuscript received 26 June 2014; revised manuscript accepted 19 September 2014. Published online ahead of print 22 October 2014. Discussion on this paper closes on 1 April 2015, for further details see p. ii.

* Geotechnical Research Institute, College of Civil and Transportation Engineering, Hohai University, Nanjing, China
† University of Plymouth, Plymouth, UK.

modelled using an assumed uniform stress, and subsoil support is present (modelled using springs), and carries a significant amount of the embankment load.

The implementation of the Hewlett and Randolph approach in BS 8006 was modified in a 2012 'Corrigendum' (BSI, 2012). This paper considers BS 8006 predictions of reinforcement tension derived from the Marston and the Hewlett and Randolph approaches as a basis for embankment load on the reinforcement, for a wide range of piled embankment geometries. The predictions are compared with results from three-dimensional FE analyses where the reinforcement is modelled as a biaxial (not isotropic or axisymmetric) material. In keeping with BS 8006, concepts of reinforcement behaviour are not further extended to separate orthogonal layers of reinforcement (e.g. Love & Milligan, 2003). Predictions of maximum sag for the reinforcement are also considered.

The effect of the side slopes of the embankment are not considered (noting that this is considered separately in BS 8006). Corresponding to the approach adopted in BS 8006, it is assumed that there is no support from the underlying subsoil.

CALCULATION OF REINFORCEMENT TENSION IN BS 8006

Embankment arching

Key geometrical variables in consideration of arching are (Fig. 1(a)): a, the pile cap size; s, the centre-to-centre pile spacing; and H, the embankment height. Here the pile geometry will refer to square caps on a square grid (i.e. a three-dimensional situation), referred to as the 'most commonly used in practice' in BS 8006.

Historically BS 8006 considered arching in a piled embankment based on an interpretation of the Marston equation for 'projecting subsurface conduits'. The 2010 revision included an alternative method for arching proposed by Hewlett & Randolph (1988), based on specific consideration of arching in a piled embankment.

Hewlett and Randolph introduced the concept of arching 'efficacy', E, referred to as 'efficiency' in BS 8006. E is defined as 'the proportion of the embankment weight carried by the piles, hence the proportion carried by the geosynthetic reinforcement may be determined as $(1 - E)$' (BS 8006 (BSI, 2010)). In fact this statement will be qualified here as 'the weight transferred to the piles *directly by arching*', since the remaining weight carried by the reinforcement is also ultimately transferred to the piles. Furthermore, there are two methods for calculation of E (failure at the 'crown' of the arch or pile cap), and hence the minimum value $E_{\min}$ is used.

Here, a nominal vertical stress acting on the reinforcement, σ_r, will be defined (noting that this is not explicitly used in BS 8006). It follows from vertical equilibrium (with no subsoil support) that

$$\sigma_r = (\gamma H + w_s)(1 - E_{\min})\frac{s^2}{s^2 - a^2} \tag{1}$$

Omitting partial load factors f, γH is the nominal vertical stress due to the embankment self-weight, and w_s is the surcharge at the surface (taken as zero in this study), both acting on plan area s^2. The reinforcement vertical stress acts on area $(s^2 - a^2)$. Love & Milligan (2003) give formulae for the reinforcement vertical stress σ_r (which they refer to as p_r) which avoid ('bypass') the use of E.

Subsoil support

Although complete loss of support from the subsoil may be considered conservative under some circumstances, it is robust, and implicit in BS 8006. However, this assumption can cause difficulty in comparison with field studies. For instance Briancon & Simon (2012) report a field study where the compressibility of the subsoil 'was not very high', and consequently the results indicate that the subsoil carries quite significant load, while the reinforcement strain is less than 1%. Almeida *et al.* (2007) describe a field study where excavations were performed under the geogrid to remove subsoil support. However, the embankment height was low (1·3 m).

As noted by Van Eekelen *et al.* (2011) 'a considerable degree of subsoil support has been measured in the available field studies ... Although this support was measured during monitoring, it may disappear in future years.' The long-term loss of support will most obviously be associated with dissipation of initial excess pore pressures (i.e. consolidation and associated settlement). There are also potential issues with future fluctuations in the groundwater table, or the presence of imported fill material below pile cap level, which will load the subsoil directly (unaffected by arching above the pile caps).

Determination of W_T

In the absence of subsoil support the tensile reinforcement will be required to carry any load not transferred to the pile caps by arching in the embankment (e.g. below the arch in Fig. 1(a)). Thus determination of the reinforcement load in BS 8006 begins with consideration of embankment arching.

BS 8006 (BSI, 2012) presents three methods for calculation of the distributed (vertical) load acting on the extensible reinforcement (W_T, kN/m; Fig. 1(b), figure 79 in BS 8006), by way of

(*a*) Marston's formula
(*b*) Hewlett & Randolph (1988) approach
(*c*) a minimum value ($W_{T\min}$).

Both (*a*) and (*b*) were referred to in the section on embankment arching, above. In fact the predictions do not relate exclusively to the named methods, since they are only used to consider arching in the embankment, and additional assumptions (below) are required to proceed to an assessment of reinforcement tension. Nevertheless, it will be convenient to refer to the methods using this nomenclature. Method (*c*) was introduced in BS 8006 (BSI, 2010).

The detailed implementation of the formulation for W_T in BS 8006 has been the subject of discussion beyond assumptions related to arching behaviour in the embankment and loss of subsoil support. For instance, W_T will not be uniform. Also, how is the vertical load from the arching embankment 'distributed' as load on the reinforcement (Love & Milligan, 2003)? Van Eekelen *et al.* (2011) argued that the approach used in BS 8006 can be modified to reduce W_T in this respect, and this appears to reflect the BS 8006 (BSI, 2012) Corrigendum as applied to the Hewlett & Randolph (1988) approach.

Using the nominal vertical stress acting on the reinforcement (σ_r) defined in equation (1), the equations for W_T based on the Hewlett and Randolph approach in the 2010 and 2012 versions of BS 8006 can be written as

$$W_T = s\sigma_r \tag{2a}$$

and

$$W_T = \frac{1}{2}(s + a)\sigma_r \tag{2b}$$

respectively.

Given that $s > a$, the more recent approach is less conservative (e.g. a 30% reduction in W_T is implied for $s/a = 2{\cdot}5$). Use of the Hewlett & Randolph (1988) method

to determine σ_r does not change, but W_T in BS 8006 is affected by the 2012 Corrigendum.

Equations (2a) and (2b) correspond to those proposed by Love & Milligan (2003) for 'transverse (lower layer)' and 'average' allocations of vertical loading on orthogonal layers of reinforcement, respectively. Love and Milligan also proposed that W_T for 'longitudinal' (upper layer) reinforcement could be calculated as $a\sigma_r$, noting that this would be less than the lower layer. Thus vertical equilibrium is satisfied by W_T corresponding to equation (2b) in both directions, but not equation (2a).

Equation (2a) is not current in BS 8006 and does not correspond correctly with vertical equilibrium as an average reinforcement value. Nevertheless, it will be considered here since the updated version in equation (2b) is less conservative.

Determination of T_{rp}

Once W_T has been determined, BS 8006 (BSI, 2010, 2012) provides a formula for calculation of tension in an extensible reinforcement (T_{rp}, kN/m run, section 8.3.3.9 of the standard)

$$T_{rp} = W_T \frac{(s-a)}{2a}\left(1+\frac{1}{6\varepsilon}\right)^{0\cdot5} \tag{3}$$

There are two unknowns: T_{rp} is the tensile load in the reinforcement (kN/m) and ε is the strain in the reinforcement.

As strain (and sag) increases the ratio T_{rp}/W_T reduces. BS 8006 states that the equation may be solved by 'the maximum allowable strain in the reinforcement and by an understanding of the load/strain characteristics of the reinforcement'. Normally it will be possible to assign the reinforcement an appropriate long-term secant stiffness (J, MN/m), which should make due allowance for creep. Then $T_{rp} = J\varepsilon$, allowing solution of the equation

$$T_{rp} = W_T \frac{(s-a)}{2a}\left(1+\frac{J}{6T_{rp}}\right)^{0\cdot5} \tag{4}$$

Given that T_{rp} appears on both sides of the equation, some iteration is required, but this can be easily automated on a personal computer.

In fact, for typical strains ($1/6\varepsilon$) is quite large compared to 1 (but less so as ε increases), and the equation can be approximated as

$$T_{rp} \approx 0\cdot35J^{1/3}\left[W_T\left(\frac{s-a}{a}\right)\right]^{2/3} \tag{5}$$

This approximation is *not* conservative in estimation of T_{rp} (e.g. 12% too low for $\varepsilon = 5\%$, increasing with ε). However, it may be useful for a rough estimate not requiring iteration. A corresponding estimate of strain is

$$\varepsilon = \frac{T_{rp}}{J} \approx 0\cdot35\left[\frac{W_T}{J}\left(\frac{s-a}{a}\right)\right]^{2/3} \tag{6}$$

This reveals that (based on this approach) tension and strain vary as $W_T^{2/3}$, while strain in the reinforcement varies as $(1/J)^{2/3}$ (noting that W_T is independent of J).

FINITE-ELEMENT ANALYSES

Finite-element mesh and analyses

Zhuang *et al.* (2012) report three-dimensional FE modelling of arching in a piled embankment, carried out using the software package 'Abaqus' (version 6.6). The analyses reported here are essentially an extension of this work, with the addition of a single layer of biaxial reinforcement near the base of the embankment.

The FE mesh is a simple cuboid $s/2$ square in plan and H high. This represents the embankment corresponding to one-quarter of a pile cap (Fig. 2). The embankment fill was modelled as a dry, linear, elastic-perfectly plastic, granular soil (Table 1, also corresponding to Zhuang *et al.*, 2012).

The base of the embankment mesh is supported rigidly by the pile cap, and elsewhere by a uniform 'subsoil stress'. The pile and subsoil are modelled by way of these boundary conditions, again corresponding to Zhuang *et al.* (2012). The subsoil stress is used to control the analysis, starting at the nominal overburden value (γH), and reducing to stimulate arching in the embankment and sag of the reinforcement. With the inclusion of reinforcement, it was possible effectively to reduce the subsoil stress to zero (or in fact a small value corresponding to the 100 mm thickness of embankment material below the reinforcement, Fig. 2). This loss of subsoil support is broadly analogous to consolidation of the subsoil with time after construction.

The FE analyses reported by Zhuang *et al.* (2012) only considered arching in the embankment (without reinforcement). The results showed reasonable correspondence with predictions from the Hewlett & Randolph (1988) method, which were about 40% higher than FE results – that is, a 'conservative' prediction (see Fig. 4(a) in the paper by Zhuang *et al.* (2012)). The importance of the mechanism of failure 'at the pile cap' (punching into the base of the embankment) was also confirmed, noting that this is not considered in the Marston approach in BS 8006.

Table 2 shows the significant range of geometries considered in this paper. Generally $a = 1\cdot0$ m, but $0\cdot5$ m is also considered. The 'spacing ratio' (s/a) increases from $2\cdot0$ to $3\cdot5$, corresponding to area ratio reducing from 25% to 8%. The height ratio $H/(s-a)$ has minimum value $2\cdot0$ to allow a 'full' arch to form (see Fig. 4(b) in the paper by Zhuang *et al.* (2012)), while the maximum height is $10\cdot0$ m.

The 'standard' size of 20-noded, reduced-integration, quadratic brick solid elements (C3D20R) was expressed as a multiple of the (smallest) length scale, l (Table 2), as shown in Table 3. The vertical dimension of elements was twice the horizontal, and elements in the 'upper' portion of the embankment (height $> 2(s-a)$) were twice the dimension of elements in the 'lower' portion (where height $< 2(s-a)$ and the main effect of arching occurred). The smallest elements were $20\cdot8$ mm (horizontal) $\times$ $41\cdot7$ mm (vertical) in the lower part of the embankment when $s = 1\cdot25$ m. The largest elements were 100 mm (horizontal) $\times$ 200 mm (vertical) in the upper part of the embankment when $s = 3\cdot5$ m.

The reinforcement was modelled using four-noded, full-integration, three-dimensional membrane elements (M3D4), which have tensile stiffness, J (MN/m), without bending stiffness. The interface with the embankment material was modelled as 'rough' (i.e. $\delta_i = \phi' = 30°$). The reinforcement was modelled as 'biaxial', using an orthotropic material with non-zero stiffness only in the orthogonal directions along the square 'grid' of pile caps. Two separate 'upper' and 'lower' orthogonal layers were not modelled, and hence the result corresponds to an 'average', which would be more than an upper layer and less than a lower layer (Love & Milligan, 2003).

Meshes contained approximately 25 000–70 000 elements. The sensitivity to mesh size was checked for each value of s using the intermediate embankment height (and low reinforcement stiffness where this was varied). l was reduced by a factor (3/4) – that is, increasing the number of elements by a factor $(4/3)^3 = 2\cdot4$. This caused the maximum tension

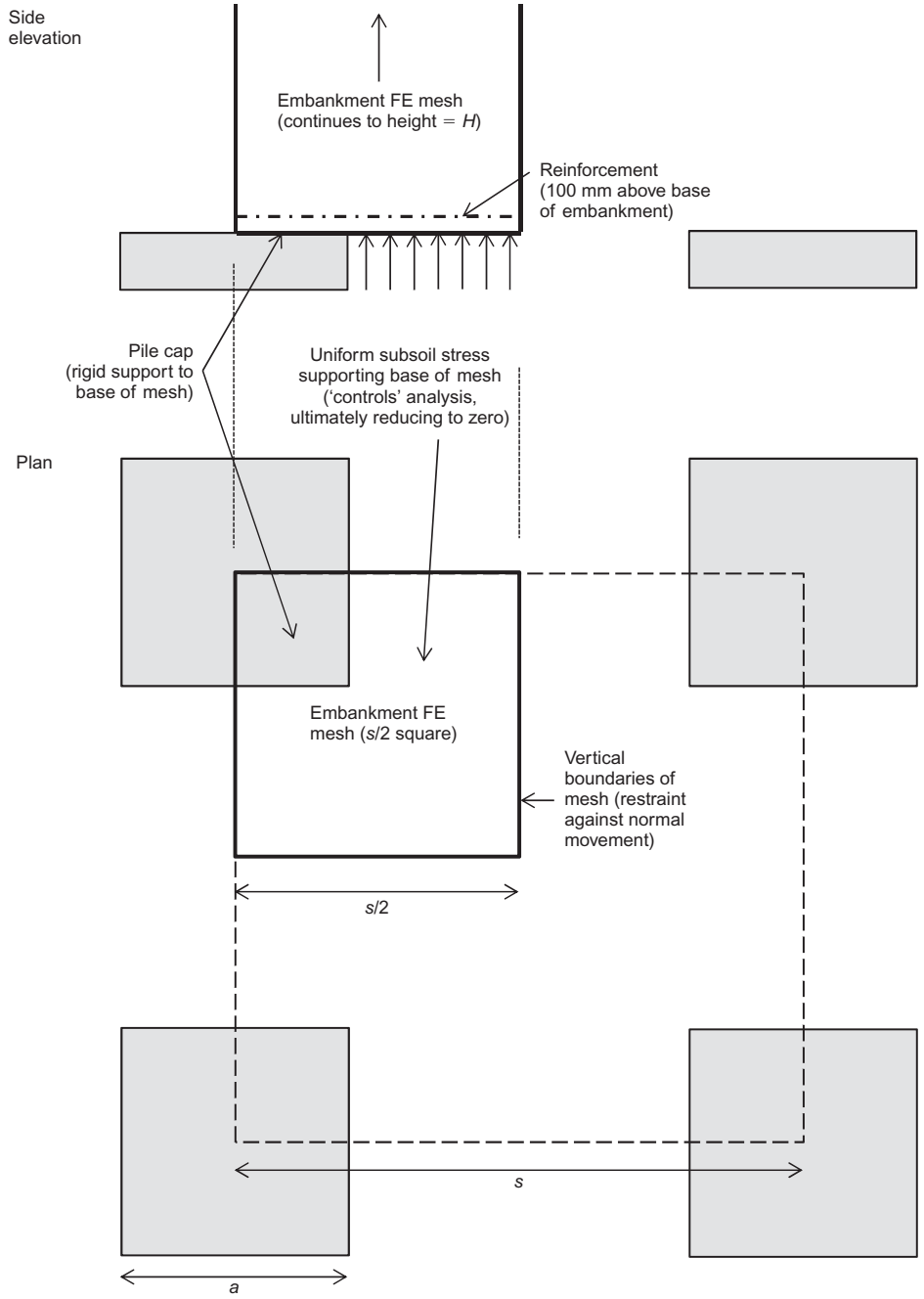

Fig. 2. Geometry and mesh boundaries

Table 1. Material parameters for embankment fill

Unit weight, γ: kN/m^3	Initial earth pressure coefficient, K_0	Young's modulus: MN/m^2	Poisson's ratio, ν	Cohesion intercept, c': kN/m^2	Friction angle, ϕ': degrees	Kinematic dilation angle at yield: degrees
17·0	0·50	25	0·20	1	30	0

in the reinforcement to increase by between 1 and 4%, while the maximum sag reduced between 1 and 3% – values which were considered suitably small.

Comparison of isotropic and biaxial reinforcement

An initial assessment was carried out to check that the biaxial reinforcement behaved as expected when compared to a (more straightforward) isotropic material. This is the only situation where isotropic reinforcement is considered.

Figure 3 shows comparison of the biaxial and isotropic reinforcement response (for $a = 1{\cdot}0$ m, $s = 2{\cdot}5$ m, $H = 6{\cdot}5$ m, $J = 3{\cdot}0$ MN/m). The horizontal axes (x, y) show normalised distance between the pile caps' centres, and hence the corners of the plot are pile cap centres. In fact only one-quarter of this area was modelled, but this has been used to produce a 'full' plot. The corners of the pile caps are at (0·2, 0·2), (0·2, 0·8), and so on, on the horizontal axes.

Subplots Figs 3(a) and 3(b) show tension in the reinforcement (biaxial and isotropic respectively) in the x-direction.

Table 2. Geometries for FE analyses

Pile cap, a: m	C–C spacing, s: m	Clear spacing, $s - a$: m	Spacing ratio, s/a	Embankment height, H: m		Height ratio, $H/(s - a)$		FE mesh length scale, l: mm
				Min.	Max.	Min.	Max.	
1·0	2·0	1·0	2·0	2·0	10·0	2·0	10·0	33·3
0·5	1·25	0·75	2·5	1·5	6·5	2·0	8·7	20·8
1·0	2·5	1·5	2·5	3·0	10·0	2·0	6·7	41·7
1·0	3·5	2·5	3·5	5·0	10·0	2·0	4·0	50·0

Table 3. Brick element dimensions in terms of length scale l (defined in Table 2)

	Height in embankment	Element dimension	
		Horizontal	Vertical
'Upper'	$> 2(s - a)$	$2l$	$4l$
'Lower'	$< 2(s - a)$	l	$2l$

The general shape of the plots shows excellent correspondence with Halvordson *et al.* (2010) and Jones *et al.* (2010) respectively. Most notably the localised 'spike' at the corner of the pile cap is most pronounced for the isotropic case, and in this case gives a maximum tension which is 22% higher than the biaxial case.

Subplots Figs 3(c) and 3(d) show vertical displacement ('sag') of the reinforcement (biaxial and isotropic respectively). The biaxial reinforcement shows maximum sag 33% higher than the isotropic reinforcement. This can be logically attributed to the 'loss' of stiffness for the biaxial material compared to the isotropic case.

RESULTS FOR REINFORCEMENT TENSION

Figure 4 compares the predictions of T_{rp} from equation (4) with the maximum tension from the FE analyses (with biaxial reinforcement). All plots show variation with embankment height, H. The four rows correspond to the values of a and s in the rows of Table 2.

The columns show different values of biaxial reinforcement stiffness, J (= 1·0, 3·0 or 10 MN/m). In general, higher J has been considered for larger clear spacing ($s - a$), and for the largest value of ($s - a$) only the highest J has been considered. The values of J represent a wide range of practical values, which are plausible in each case based on equation (4).

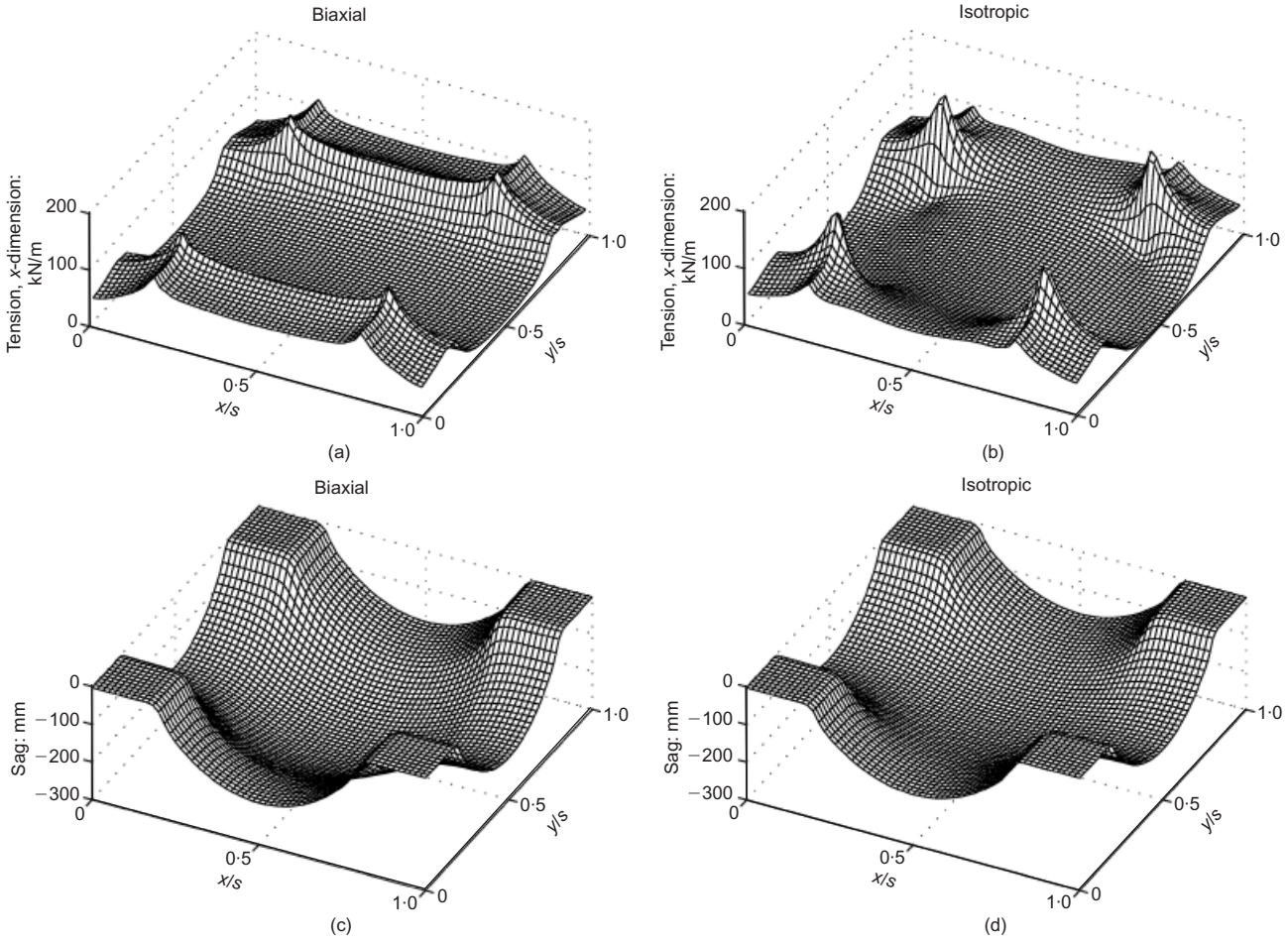

Fig. 3. Comparison of biaxial and isotropic reinforcement tension and sag ($a = 1·0$ m, $s = 2·5$ m, $H = 6·5$ m, $J = 3·0$ MN/m). Horizontal axes show normalised distance between pile cap centres

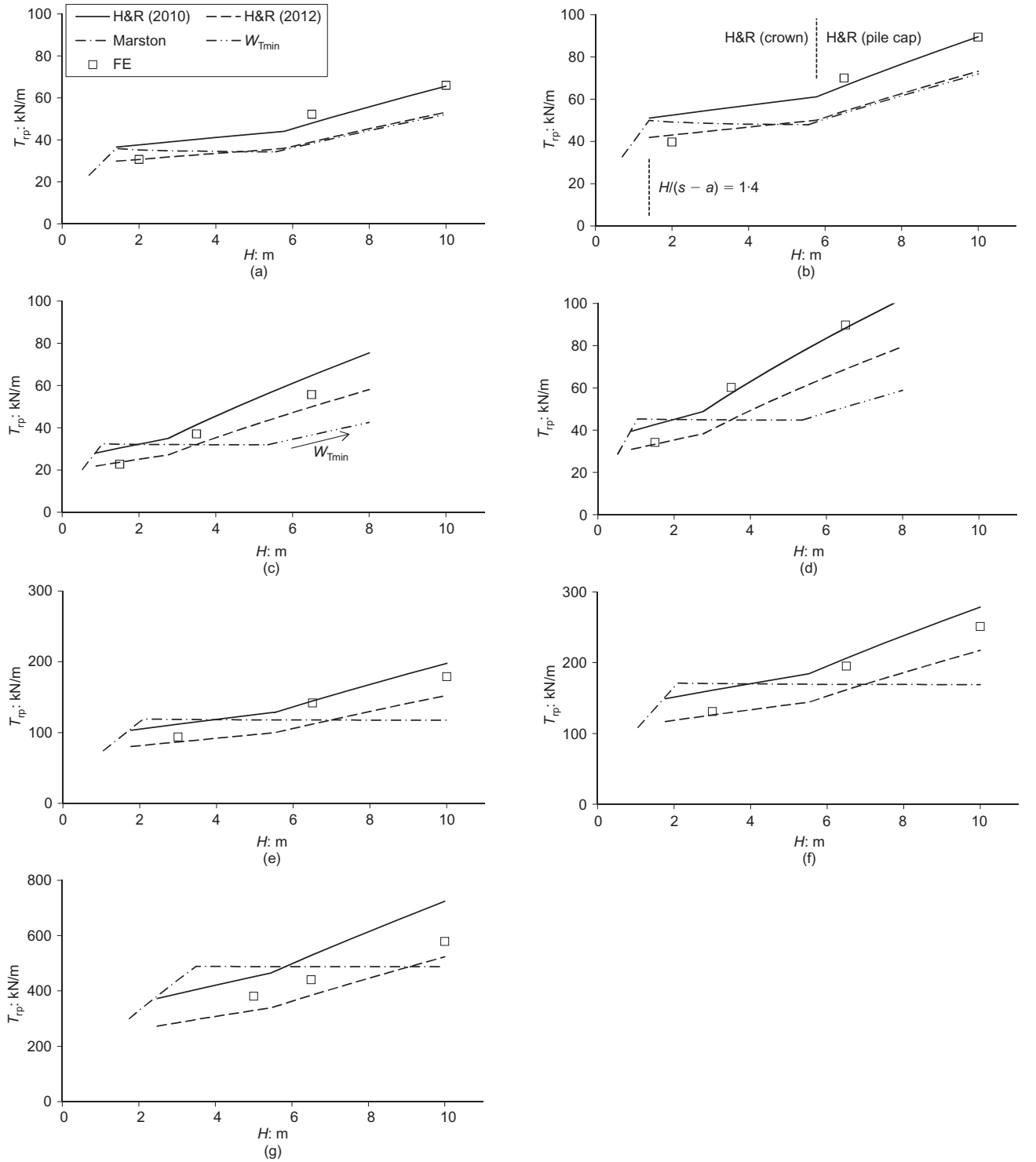

Fig. 4. Variation of reinforcement tension (T_{rp}) with embankment height (H): predictions and FE results (a) $a = 1{\cdot}0$ m; $s = 2{\cdot}0$ m; $J = 1{\cdot}0$ MN/m; (b) $a = 1{\cdot}0$ m; $s = 2{\cdot}0$ m; $J = 3{\cdot}0$ MN/m; (c) $a = 0{\cdot}5$ m; $s = 1{\cdot}25$ m; $J = 1{\cdot}0$ MN/m; (d) $a = 0{\cdot}5$ m; $s = 1{\cdot}25$ m; $J = 3{\cdot}0$ MN/m; (e) $a = 1{\cdot}0$ m; $s = 2{\cdot}5$ m; $J = 3{\cdot}0$ MN/m; (f) $a = 1{\cdot}0$ m; $s = 2{\cdot}5$ m; $J = 10$ MN/m; (g) $a = 1{\cdot}0$ m; $s = 3{\cdot}5$ m; $J = 10$ MN/m

The predictions from equation (4) are shown as continuous variation with embankment height, H. For direct comparison with the FE analyses, partial load factors (f) have been taken as 1, and the surcharge (w_s) is 0.

For the Marston prediction of W_T the piles were assumed to be 'normal' (rather than 'unyielding'), noting that this gives a more conservative (higher) value (e.g. Ellis & Aslam, 2009). For the Hewlett and Randolph (H&R) approach the passive earth pressure coefficient K_p was taken as 3·0, corresponding to $\phi' = 30°$ for the embankment fill in the FE analyses (Table 1). 'H&R (2010)' and 'H&R (2012)' refer to equations (2a) and (2b) respectively, noting that σ_r follows directly from the original method and does not change. The W_{Tmin} limit ($= 0{\cdot}15\gamma sH$ for $f = 1$ and $w_s = 0$) was also applied where relevant.

As illustrated in Fig. 4, changes in the response are observed for the Marston approach when $H/(s - a) = 1{\cdot}4$ (Fig. 4(b)), and when the W_{Tmin} limit is applicable for higher embankments (Fig. 4(c)). As $(s - a)$ increases the W_{Tmin} limit does not have an effect (Figs 4(e)–4(g)).

For the Hewlett and Randolph approach there is a transition from criticality of failure at the crown of the arch to the pile cap as embankment height increases (Zhuang *et al.*, 2012), and the W_{Tmin} limit does not take effect for any of the geometries considered. Predictions of T_{rp} from H&R (2012) are between 18 and 28% smaller than H&R (2010), where the difference increases with (s/a).

The increase in J between the two columns results in a reduction in implied reinforcement strain (equation (6)). Taking a nominal allowable strain of 5%, T_{rp} is 50, 150 and 500 kN/m for $J = 1{\cdot}0$, $3{\cdot}0$ or 10 MN/m respectively. The values predicted illustrate that the combinations of geometry and stiffness are broadly sensible. For example, $T_{rp} > 50$ kN/m for large H in Fig. 4(a), but $T_{rp} < 150$ kN/m for all H in Fig. 4(b).

The FE results are shown by discrete data points at three values of H on each plot. In general, agreement with the Hewlett and Randolph approach is good: the 2010 and 2012 approaches appear to give upper and lower bounds respectively. This is perhaps surprising since

(*a*) the Hewlett and Randolph method overpredicts vertical stress in the arching embankment compared to FE analysis (Zhuang *et al.*, 2012)
(*b*) equation (2a) is not consistent with vertical equilibrium
(*c*) equation (3) does not specifically account for non-uniform stress in the reinforcement (Fig. 3(a)), and is thus likely to underpredict T_{rp}
(*d*) there is uncertainty regarding the relationship linking T_{rp} and W_T (e.g. equations (2a) and (2b)).

In fact it would appear that the net effect is (perhaps fortuitously) approximately neutral compared to the FE analyses. It is also potentially concerning that the current revision of BS 8006 somewhat *underpredicts* the data.

Concerns regarding underprediction from the Marston method as H increases appear to be confirmed (e.g. Ellis & Aslam, 2009; Van Eekelen *et al.*, 2011), although the W_{Tmin} limit mitigates this effect to some extent. Agreement for the Marston method (and the W_{Tmin} limit) is certainly not as good as the Hewlett and Randolph method.

RESULTS FOR REINFORCEMENT SAG

Section 8.3.3.14 in BS 8006 (BSI, 2010, 2012) also suggests that the maximum sag in the reinforcement (y) spanning between pile caps can be estimated as

$$\frac{y}{s-a} = \left(\frac{3\varepsilon}{8}\right)^{0{\cdot}5} \tag{7}$$

This equation is based on a span ($s - a$), rather than the diagonal, which is $\sqrt{2}$ times longer (Fig. 2). The maximum sag is (unsurprisingly) observed on the diagonal Figs 3(c) and 3(d), and thus using $(s-a)\sqrt{2}$ in place of $(s - a)$, and again assuming that $\varepsilon = (T_{rp}/J)$

$$\frac{y}{s-a} = \sqrt{2}\left(\frac{3\varepsilon}{8}\right)^{0{\cdot}5} = \left(\frac{3T_{rp}}{4J}\right)^{0{\cdot}5} \tag{8}$$

BS 8006 actually suggests a factor of 2 (rather than $\sqrt{2}$) be applied to equation (7) when considering sag on the diagonal. This would give predictions of normalised sag $\sqrt{2}$ times higher than equation (8). Love & Milligan (2003) note that, for separate orthogonal layers, the maximum sag would result from addition of sag in the layers.

For reinforcement strain in the range 3–6% equation (8) predicts normalised sag in the range 15–21%.

Hence normalised maximum sag $y/(s - a)$ was predicted using equation (2a) for W_T, equation (4) for T_{rp}, and equation (8). Fig. 5 shows the result for each FE geometry (Table 2), compared with the corresponding FE results. Where two values of J were used for a given geometry (Fig. 3), 'filled' (or 'solid') data points are used for the higher value, and thus these points have lower sag. The range of data spans (exceeds) the range of 15–21% mentioned above. Agreement is good, with error up to ±20% in the prediction from equation (8) compared with the FE results. As expected, using equation (2b) instead of equation (2a) led to a reduction (of 10–15%) in predicted sag, and thus agreement was not as good.

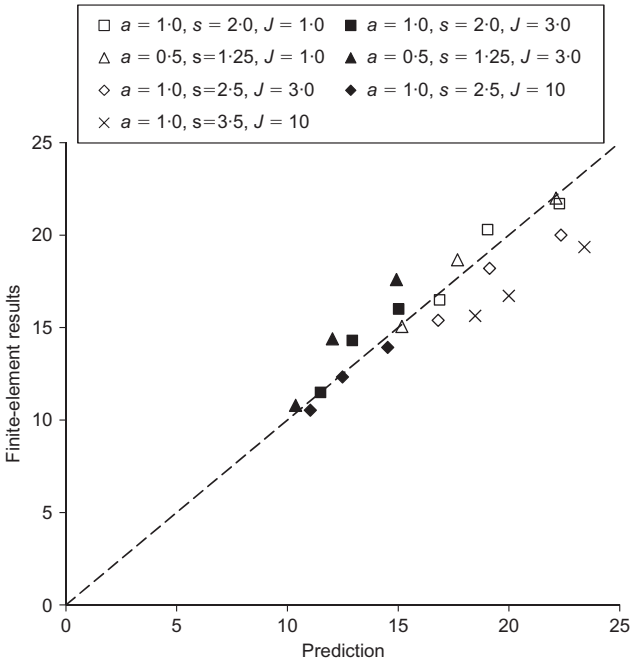

Fig. 5. Normalised maximum sag $y/(s - a)$: comparison of FE results and prediction using equations (2a), (4) and (8)

CONCLUSIONS

BS 8006 (BSI, 2012) allows prediction of reinforcement tension in a piled embankment using the Marston and the Hewlett & Randolph (1988) approaches as a basis for embankment load on the reinforcement, and noting that the latter has been changed compared to BS 8006 (BSI, 2010). This paper presents predictions by these methods for a wide range of piled embankment geometries, and comparison with results from three-dimensional FE analyses. The analyses consider complete loss of subsoil support, and reinforcement with biaxial (not isotropic or axisymmetric) properties. However, separate 'upper' and 'lower' orthogonal layers of reinforcement (e.g. Love & Milligan, 2003) were not modelled, and hence the result corresponds to an 'average' which would be more than an upper layer and less than a lower layer (Love & Milligan, 2003).

Concerns regarding use of the Marston approach for high embankments (e.g. Ellis & Aslam, 2009; Van Eekelen *et al.*, 2011) are confirmed. However, the Hewlett and Randolph approach compares well with the FE results for all geometries, with the BS 8006 (BSI, 2010) and BS 8006 (BSI, 2012) approaches providing reasonable upper and lower bounds to the data respectively. This is perhaps surprising since it can be argued that individual component elements in the ultimate prediction appear somewhat deficient and inaccurate. It is also potentially concerning that the 2010

revision (upper bound to the data) is now superseded, and the current version is a lower bound.

A suggested modification to the BS 8006 formula for prediction of reinforcement sag also gives good agreement with the FE analyses.

ACKNOWLEDGEMENTS

The financial support of the National Natural Science Foundation of China (grant no. 51478166 and 51108155), the Scientific Research Foundation for the Returned Overseas Chinese Scholars, State Education Ministry and the Fundamental Research Funds for the Central Universities (grant no. 2014B04914) is acknowledged.

NOTATION

Please note, the notation is consistent with BS 8006 where relevant.

- a (square) pile cap size (m)
- c' cohesion intercept (kN/m^2)
- E efficiency (or 'efficacy') of arching from the Hewlett & Randolph (1988) method, dimensionless (proportion of the embankment weight transferred directly by embankment arching onto the piles)
- f BS 8006 partial load factors (taken as 1 in this study)
- H embankment height (m)
- J long-term secant stiffness (at appropriate strain) for reinforcement (kN/m run (or MN/m))
- s pile centre-to-centre spacing (for piles on a square grid) (m)
- T_{rp} maximum tensile load in reinforcement (kN/m run)
- W_T distributed (vertical) load carried by reinforcement between adjacent pile caps (kN/m)
- w_s surcharge load at surface of embankment (taken as 0 in this study) (kN/m^2)
- y maximum sag in reinforcement (m)
- ε strain in reinforcement
- ν Poisson ratio
- σ_r vertical stress acting on reinforcement (kN/m^2)
- ϕ' friction angle (degrees)

REFERENCES

Almeida, M. S. S., Ehrlich, M., Spotti, A. P. & Marques, M. E. S. (2007). Embankment supported on piles with biaxial geogrids. *Proc. Instn Civ. Engrs – Geotech. Engng* **160**, No. 4, 185–192.

Briancon, L. & Simon, B. (2012). Performance of a pile-supported embankment over soft soil: a full-scale experiment. *ASCE J. Geotech. Geoenviron. Engng* **138**, No. 4, 551–561.

BSI (2010). BS 8006-1: Code of practice for strengthened/reinforced soils and other fills. London, UK: British Standards Institution.

BSI (2012). BS 8006-1: Code of practice for strengthened/reinforced soils and other fills, incorporating Corrigendum 1. London, UK: British Standards Institution.

Ellis, E. A. & Aslam, R. (2009). Arching in piled embankments: comparison of centrifuge tests and predictive methods – part 1 of 2. *Ground Engng* **42**, June, 34–38.

Halvordson, K. A., Plaut, R. H. & Filz, G. M. (2010). Analysis of geosynthetic reinforcement in pile-supported embankments. Part II: 3D cable-net model. *Geosynthetics Int*. **17**, No. 2, 68–76.

Hewlett, W. J. & Randolph, M. F. (1988). Analysis of piled embankments. *Ground Engng* **21**, April, 12–18.

Jones, B. M., Plaut, R. H. & Filz, G. M. (2010). Analysis of geosynthetic reinforcement in pile-supported embankments. Part I: 3D plate model. *Geosynthetics Int*. **17**, No. 2, 59–67.

Liu, H. L., Ng, C. W. W. & Fei, K. (2007). Performance of a geogrid-reinforced and pile-supported highway embankment over soft clay: case study. *ASCE J. Geotech. Geoenviron. Engng* **133**, No. 12, 1483–1493.

Love, J. & Milligan, G. (2003). Design methods for basally reinforced pile-supported embankments over soft ground. *Ground Engng* **39**, March, 43–43.

Plaut, R. H. & Filz, G. M. (2010). Analysis of geosynthetic reinforcement in pile-supported embankments. Part III: Axisymmetric model. *Geosynthetics Int*. **17**, No. 2, 77–85.

Van Eekelen, S. J. M., Bezuijen, A. & van Tol, A. F. (2011). Analysis and modification of the British Standard BS 8006 for the design of piled embankments. *Geotextiles and Geomembranes* **29**, No. 3, 345–359.

Zhuang, Y., Ellis, E. A. & Yu, H. S. (2012). Technical note: Three-dimensional finite element analysis of arching in a piled embankment. *Géotechnique* **62**, No. 12, 1127–1131, http://dx.doi.org/10.1680/geot.9.P.113.